Monitoring Harness Use in Construction with BLE Beacons

Jesús M. Gómez-de-Gabriel[a], Juan A. Fernández-Madrigal[a], Antonio López-Arquillos[b], Juan Carlos Rubio-Romero[b]

[a]*System Engineering and Automation Dpt.*
[b]*Economics and Business Management Dpt.*
University of Málaga, Spain

Abstract

This paper introduces a novel approach to measure and evaluate the proper use of harnesses at construction sites:we deploy Bluetooth Low Energy (BLE) beacons for delimiting areas where the use of a harness is mandatory and to detect whether the harness is attached to the corresponding lifeline when the worker enter these areas. Our method is based on local estimation, through statistical filtering of RSSI measurements (Extended Kalman Filter),of the proximity between the beacons that delimit the different areas and the one in the lifeline, followed by a finite state machine risk status detector. Experiments have been performed in a real construction work-place with a wearable device; their results show that our solution is ideal for dynamic construction environments. Its main advantages are robustness of the detection system, easy relocation of the beacons as the construction zone evolves,and no need for calibration, communication infrastructure, external processing support, or configuration/map updates. Additionally, optional remote IoT for online monitoring is possible.

Keywords: Harness, construction safety, fall from height, beacon, sensor, safety at work.

Email address: alopezarquillos@uma.es (Antonio López-Arquillos)

Table 1: Main preventive measures against falls from height in the construction sector.

Strategy	Measure	Authors
Prevention through Design (PtD)	Safety operations included in the design of the project	[9, 10, 11]
Workers' Organization	Work planning Worker training	[13, 14, 15]
Collective measures	Safety nets Scaffolding Safety platforms	[16, 17, 18, 19, 20]
Personal protection equipment (PPE)	Safety harnesses and lifelines	[21, 22, 23]

1. Introduction

Occupational accidents in the construction sector continue to give international cause for concern [1]. In particular, falls from height have been identified as a leading cause of fatal accidents in the sector by several authors in many countries, such as the USA [2], Taiwan [3], Spain [4], China[5], Korea[6], Australia [7] or Uganda [8].Some preventive measures have been proposed to prevent falls from height, and other safety risks, which focus on different strategies. As an example, Prevention through Design (PtD) strategies are based on the inclusion of safety requirements while the project is being designed and not after the design phase [9, 10, 11, 12]. Other authors focus on workers' organization issues such as task planning or safety training [13, 14, 15]. Also, studies about collective measures [16, 17, 18, 19, 20] and personal protective equipment [21, 22, 23] try to mitigate the effects in case of accident, because prevention is not always entirely effective. A compilation of preventive strategies is shown in Table 1.

In construction, not all personal protection equipment is compulsory at every workplace, depending on the risk level in a given zone. Examples of this are harnesses and lifelines :It is not mandatory to connect them at ground level as there is no evidence of any risk of falls from height, but they are mandatory when the worker enters a dangerous zone such as a roof or top floor. According to [24], the problem is that harnesses can be available at the work site but not correctly used.

The introduction of electronic devices in the sector has contributed to improving occupational safety among construction workers. For instance, several technologies such as Radio-frequency identification (RFID) [25], Global

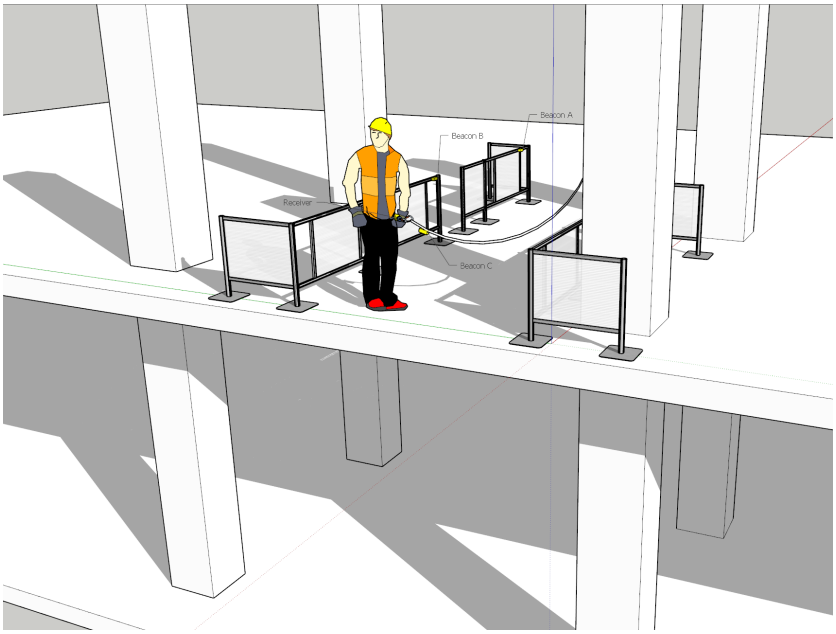

Figure 1: The detection of the use of the safety measures can be done with just three beacons. Beacons A and B are placed in the transition between a safe place and a risk area. A third beacon is located at the lifeline carabiner.

Positioning System (GPS) [26] or Ultra-wideband (UWB) [27] have served for the identification, localization and tracking of materials. More recently, similar technologies have been applied in the field of occupational safety to detect personal protection equipment and improve safety conditions [28, 29, 30].

Two main wireless technologies are used in work safety applications: RFID and radio-frequency beacons.

On the one hand, RFID tags are simple and powered just from the energy captured by their antenna. RFID solutions can be implemented to detect the presence of passive tags [31] in ranges of up to $20\,m$, depending on the frequency, antenna sizes and transmitting power. Near-field communication (NFC) is a subset in the family of RFID technology. They operate at the $13.56\,MHz$ frequency, within a range of about $30\,cm$, and they have been designed as a secure form of data exchange. An NFC device is capable of being both an NFC reader and an NFC tag. Many smartphones use this technology today for secure payments(a comparative overview of various Body Area Networks can be found in [32]).

Table 2: Comparison of localization technologies. (Adapted from Lin 2013)

	BLE (Bluetooth Low Energy)	RFID passive	RFID active	ZigBee	Wi-Fi	GPS
Power usage	Low	None	Low to medium	Medium	High	Medium
Data rate	Low	Low	Low to medium	Medium	High	N/A
Coverage	Medium	Low	Medium	High	High	Very high (outdoor)
HW costs	Low	Low	Medium	Medium	High	High
Advantages	Low price and battery powered	Low price. No battery required in tag	Low price	Low price	Popular devices (AP)	Long range coverage
Disadvantages	Low precision	Very short range	Low precision	Power consumption	High power consumption	Only outdoor workplaces
Deployability	Easy	Easy	Easy	Easy	Medium	Easy
Accuracy	Poor	Bad	Good	Good	Bad	Bad
Maintainability	Good	Good	Good	Good	Bad	Good
Stability	Good	Good	Good	Good	Bad	Good

On the other hand, the current standard in radio-frequency beacons is based on the Bluetooth 4.0 specification. It defines the Bluetooth Low Energy (BLE) protocol, that includes the advertising (i.e. beaconing) mode. In this mode, low-power devices broadcast very short messages at a configurable rate that includes the device identification number and the services offered. These messages can be read by any Bluetooth 4.0 or above compatible device without pairing. BLE beacons can continue transmitting for years with a single coin cell battery, thus they are used today as a proximity detection system in commercial, cultural and indoor shops, museums and airports.

A comparison of these and other common localization technologies is shown in Table 2. There are two main beacon protocols that provide additional functionalities to build the Physical Web[1]: proprietary protocols from specific vendors like the *iBeacon* from Apple [33], and the *Eddystone* open standard by Google. A survey on the hardware and protocols of the beacons can be found in [34].

There are solutions based on RFIDs for the detection of proximity to certain areas (e.g., [30]), but they do not perform continuous monitoring. Other limitations of RFID systems, such as the lack of accuracy and interference with materials, have been also studied in literature [35]. Considering that, our work has been based on radio-frequency.

In this paper we introduce a new sensor system for the proper use of harnesses and life-lines in workplaces where it is mandatory due to the high

[1]https://google.github.io/physical-web/

occupational risk levels of fall from height (see the illustration in Figure 1). Our system is composed of an instrumented harness with a BLE receiver, a beacon located at the lifeline carabiner hook, and a set of additional active BLE beacons placed along the risk area entry paths of the workplace. On the software side, a hybrid statistical filtering / finite state machine method deduces both the area in which the worker is located and whether the lifeline has been attached before entering a risk zone, using only the RSSI measurements of just three beacons, with minor configuration.

The main contribution of this work is thus the use of a simple wearable receiver to detect the current status of the worker, without the need of communications or powerful computing infrastructure, and without maps, only using battery-powered beacon pairs that can be easily deployed, relocated and extended as the construction environment evolves. Up to the knowledge of the authors, this is the first method that can be effectively used in construction environments for any number of workers and areas since changes can be implemented simply by the physical relocation of the beacons.

The structure of the paper is as follows. In section 2, related works are presented. Section 3 describes all the physical components of our system. Section 4 explains the filtering/state-machine method we have implemented for detecting the status of the worker with respect to the beacons. In section 5 we discuss the results obtained with our approach. Finally, in section 6 we review the work and propose some future extensions.

2. Related works

Some form of positioning technology must be implemented to track people's positions at the workplace. GPS signals are often unavailable indoors, and the accuracy of public GPS networks is still insufficient for safety applications. Private indoor location systems can use active radio-frequency transmitters at known locations; the receiver resolves its position by analysing the attenuation of the signal from each beacon. However, real environments make it difficult to obtain reliable measurements due to attenuations and distances [36].

Modern Real-time Locating Systems (RTLS) use various localization techniques, including the received signal strength indicator (RSSI), time of arrival (TOA), time difference of arrival (TDOA), and angle of arrival (AOA) [37]. We are interested here in the simplest one, RSSI, where attenuations, measured in dB over a milliwatt (dBmW or dBm) are computed in the receiver

thanks to the transmission power indications reported by the transmitter.

The most common method for estimating the worker's location from the physical measurements is based on triangulation; in that case, RSSI values are considered a function of distance [37]. The problem is that the RSSI signal is very unreliable in a construction workplace due to radio propagation disturbances.

Instead of estimating the distance to each beacon based on the theoretical RSSI-distance relationship, fingerprinting methods use a pre-built sampled map of the RSSI values from the different beacons to match the current RSSI signals pattern [36]. Here, the navigation constraints of complex indoor environments can assist these positioning methods to provide higher accuracy, compared with open environments [38].

Sensor fusion with information from several sources can provide even more accurate results. For instance, using pedestrian dead reckoning (PDR) and a set of beacons placed on a global map, a 2 m position precision has been obtained [39].

An alternative to localization are the so-called proximity methods, that are not aimed at estimating a specific location, but to assess the proximity to a special place, by using special beacons located at trucks, corridors, ladders, etc. [40]. This can also serve to check whether the worker is wearing certain equipment (with a beacon attached to it).

Besides the method used, when considering mobile or wearable solutions, size and power consumption have to be taken into account. For instance, in [41] a patent is presented of a method for reducing energy consumption in a tracking device based on the estimation of speed in RF-based localization.

The cost of deploying communication infrastructures in non-permanent areas, or the cost of using cellular data networks can be too high. This way, in [42] a method is presented that reduces the reporting of the fingerprints to the location server: the server provides zones with RSS-based representation, and the terminal reports the measurements only when the readings match the configured RSS patterns.

Finally, the particular characteristics of construction sites frequently reduce the suitability of many methods. A global view of the advantages and disadvantages of the previous methods when applied in construction sites are shown in table 3. A system for worker localization and proximity to risk areas in railway construction was proposed by D'Arco [43] based in GNSS and RSSI, but it is not recommended for indoor environments. Other authors like Park [40] have proposed to calculate the risk level of the worker

Table 3: Comparison of methods applied in construction sites.

System	New system	D'Arco (2018)	Park (2017)	Teizer (2007)	Kelm (2013)	Lin (2013)
Aplications	Detection of risk area and PPE use at any worksite	Risk areas at Railway construction	Heavy equipment proximity(trucks)	Evaluate worker training	Acces and PPE control	Worker behaviour analysis
Outputs	Worker risk status considering risk area and PPE attached	Worker location and risk area	Worker risk level	Worker position and velocity	Compliance of mandatory PPE	Worker position
Technology used	BLE (RSSI)	GNSS +RSSI	BLE (RSSI)+ Bluetooth / WIFI	UWB	RFID (Active/ Passive)	ZigBee and fingerprint
Indoor/ Outdoor	Both	Outdoor	Both	Indoor	Indoor	Both
Suitable for dynamics environments	Yes	Yes	Yes	Hard	Hard	Expensive
Continuous monitoring	Yes	Yes	Yes	Yes	No	Yes
Requires Comunication Infrastructure	None	Network	Optional	Network and server	Database access and RFID detection	ZigBee WSN
Sensitivity to calibration	Low	Low	High	Very high	None	Very high
Local/Global	Local	Global	Local	Global	Local	Global

according to the proximity and movement of heavy equipment (trucks), but with a high sensitivity of the system to calibration. Worker position and velocity were obtained in the solution based in UWB proposed by Teizer [27], although it is hard and expensive to install and calibrate, especially in dynamic environments.

The authors have not found any previous work that monitors the use of the harness and the closeness to risk zones with so little calibration and configuration effort as the one introduced in this paper.

3. Overview of the solution

In this section we describe generally our solution, its electronic components and the behavior of the RSSI signal which it is based on. The proximity detection method is detailed in section 4.

3.1. System and components

The basic arrangement of our proposal is shown in Figure 2. The wearable receiver (R), a Bluetooth Low Energy receiver with a programmable microcontroller, is attached to the worker's safety harness. Two beacons (A) and (B) are located on the side of the stairs/corridor that give access to

Figure 2: Two beacons are located in sequence on the side of the entry to the risk area (Left). A third beacon is located on the carabiner that connects the lifeline with the worker harness (Right).

the area of the workplace where there is a risk of falling. A third beacon is attached to the lifeline hook (C).

Bluetooth Low Energy is enabled by turning off the radio, using low standby time, a fast connection and low peak power. The spectrum for Bluetooth extends from 2.402 MHz to 2.480 MHz with 40 1 MHz-wide channels, numbered 0 to 39, separated by 2 MHz. Channels 37, 38, and 39 are the only ones used for sending advertisement packets periodically. The time interval between packets has both a configurable fixed interval and a random delay to reduce the collision probability between advertisements from different devices [44].

Beaconing devices from Bytereal Telecommunications International Limited (HongKong) have been employed in our experiments (See Figure 3). Based on the Texas Instruments cc2541, these devices are small and provide BLE with configurable parameters via a mobile application for Android/IOs. They can operate on single coin cell battery (CR2477) for more than one year, although their effective life depends on the configured advertising rate.

The wearable BLE receiver is based on the powerful and inexpensive ESP32 chip-set (Espressif Systems, Shanghai, China)[2], which was designed

[2]https://www.espressif.com/en/products/hardware/esp32/overview

Figure 3: BLE Beacons used in the experiments and a view of the circuit (Left). The receiver (right) is based on an ESP32 chip from Espressif, with Wi-Fi and Bluetooth communications, and powered with a 18650 Li-ion battery. The detection of the lifeline attachment is possible thanks to a commercial BLE beacon placed near the carabiner.

for IoT applications. The ESP32 features a Hybrid Wi-Fi and Bluetooth Chip ESP32 with in-built antenna switches, RF components, and power management modules. It is low power and capable of reliable operation in industrial environments within a wide temperature range (see Figure 3).

There is an official open source software development kit in a public repository for the programming of the device using the Arduino IDE that includes Bluetooth Low Energy libraries and examples[3]. The *BLEScan.cpp* software module has been modified in this work to change its discovery behaviour in toder to provide continuous scan. Other libraries provide support for Wi-Fi communications and MQTT protocol functions (Message Queuing Telemetry Transport) to implement an Internet of Things (IoT) device.

3.2. RSSI measurements

The BLE API functions provide RSSI values of power for the advertising messages received during the scan phase. The ESP32 has been programmed to keep scanning continuously these signals coming from the known beacons (e.g. Beacons A, B and C) and storing them into a FIFO buffer.

RSSI values are noisy and depend on the environment objects and electromagnetic interferences, suffering effects such as reflection, refraction, diffrac-

[3]https://github.com/espressif/arduino-esp32/tree/master/libraries

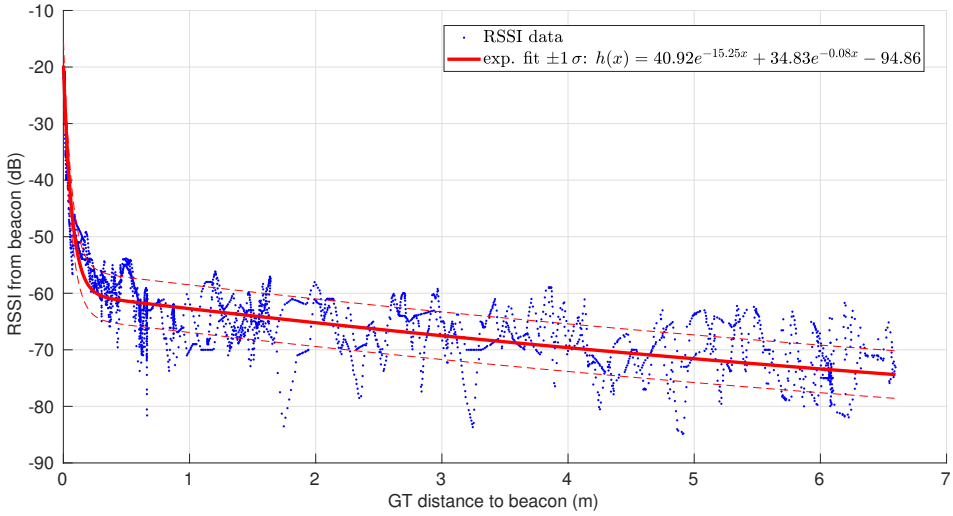

Figure 4: RSSI readings vs. ground-truth distances provided by LIDAR in a scenario where we moved away from the beacon and then came back —hence the two overlapped blue curves of measurements. A theoretical sensor model based on a homoskedastic double exponential fit to the data is also shown: $h(x) = ae^{bx} + ce^{dx} - o$.

tion, and scattering. Also, misalignments between the beacon and the receiver antenna cause polarizations [45].

In Fig. 4 a scatter plot of $\simeq 800$ RSSI values gathered from our beacons at distances from 0 to $5\,m$ is shown, along with a theoretical exponential model of these sensors.

Elsewhere [46], a different model has been used for reporting a relationship between RSSI values and distances:

$$RSSI(d) = RSSI(d_0) - 10\,n\,log_{10}(d/d_0) \tag{1}$$

which can be considered a two-parameters equation, where $RSSI(d_0)$ is the RSSI level measured at $d_0 = 1\,m$ distance and n is the attenuation parameter. Those parameters are easy to identify from specific beacons in specific environments; however, this is not suitable for dynamic environments such as construction, since the RSSI-to-distance conversion is hard to implement and parameters are changing all the time. Because of this, we use directly the RSSI values and their previously explained exponential model into the

filters of section 4.1 to detect proximity to the beacons.

Notice that the different channels will exhibit different attenuations, and thus, different base levels for the RSSI measurements. One of the reasons for the attenuation differences between channels is the multipath interference [47]. This attenuation may change with the distance in up-to -30 dBm in just 10 cm displacements. A beacon transmits every advertising message in the three channels (37, 38 and 39), and a BLE scanner listens in one of these channels sequentially in every scan. BLE libraries do not provide information about the channel used for the received messages, but if the advertising interval matches the scan period (as we do), a sequence of readings is obtained where the same channel is used every three packets, which allow us to address the different attenuation problem.

Also notice that the requirements of the application involve a moving target that has to be tracked (the worker), which may lead to additional constraints in the advertising rate of the beacons. As the default scan interval of the wearable receiver is 100 ms, an advertising rate of 100 ms has been selected for all our beacons. Then, a moving window over the last three readings, from which the signal with minimum attenuation is chosen, has been used successfully to get only one RSSI value at a time with consistent attenuation level.

4. Description of the method

In order to detect the worker status, a proximity detection filter (subsection 4.1) plus a Finite State Machine (FMS) model of the worker status (subsection 4.2) have been developed and interconnected specifically for this problem.

4.1. Development of the proximity detection filter

Fig. 5 shows the dynamic Bayesian network (DBN) associated to the estimation problem of the proximity to one beacon when we assume Markovianity both in metrical distances and in discrete regions —close/far —w.r.t. a beacon. The random variable r_i represents RSSI measurements, and the two hidden variables d_i and c_i, respectively, the true metrical distance from the worker to the beacon and the belief in the region where the worker is —what we ultimately want to estimate. The variable z_i is required in order to formulate a recursive filter for c_i and it will be explained further on.

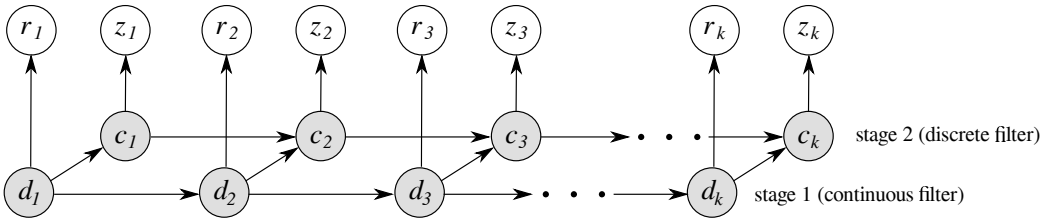

Figure 5: Dynamic Bayesian network for the stochastic processes that govern the changes in the distances of the worker to a beacon (d_i, meters) and in the regions where the worker is believed to be (c_i, far from or close to the beacon). We have also indicated hidden variables (shadowed) and visible variables (not shadowed)

Notice that c_i is not a mere consequence of being at a given metrical distance d_i, but a belief in being close or not to the beacon, something that also depends on our previous belief c_{i-1} (because it would be unlikely that the worker leaves and enters the "closeness region" many times in a too short period of time). Also note that if we wish to use the dependencies between c_i and c_{i-1} and also keep Markovianity, we need to know (estimate) d_i due to the structure of this DBN and how d-separation works [48]; otherwise, $c_i \not\perp c_{1:i-2}|c_{i-1}$. Thus the correct Markovian estimation of c_i in this DBN must rely on conditioning to d_i.

We separate the estimation of the hidden state —the pair (d_k, c_k) into two parts, each one being solved by a different filter: the first stage is a Gaussian filter that estimates d_k using observations $r_{1:k}$, while the second is a discrete filter that uses the results of the first stage for estimating c_k, our final goal (thus satisfying our condition that we know d_i when estimating c_i). Although we lose some information about the inter-relations between d_i and c_i due to this being an approximation to Rao-Blackwellization [49], we have found that the resulting uncertainty is kept within reasonable limits. This is also an efficient solution, since the first filter can be implemented with an EKF [50] (an Extended Kalman Filter is required because the observation model, as it was shown in Fig. 4, is non-linear).

In order to set up this double filter, the second stage —the discrete filter needs some non-hidden observation to do its estimations. We do not have such a "sensor", but when we are estimating c_i we have already estimated d_i, therefore we can approximate the missing sensor by generating "virtual observations" z_i from the estimates of the first filter. We have chosen the z_i variables to be the probability of the estimate EKF_i to be closer than a

given threshold τ_c from the beacon($z_i = cdf_{EKF_i}(\tau_c)$). We have used 70 cm for that threshold ($\tau_c = 0.7$) in our experiments after checking out that the worker never gets closer than 60 cm to the beacons.

With all these considerations, we can now formulate both filters. The first stage (EKF) is governed by the following system state model:

$$\begin{aligned} &d_k = d_{k-1} + \epsilon_k, \quad \epsilon_k \sim N(\epsilon_k; 0, Q_k) \\ &r_k = h(d_k) + \delta_k, \quad \delta_k \sim N(\delta_k; 0, R_k), \quad \epsilon_k \perp \delta_k \\ &h_k(x) = ae^{bx} + ce^{dx} - o \end{aligned} \tag{2}$$

where $h()$ is the observation model, i.e., the exponential that we depicted in Fig. 4. Note that the dynamics of this system does not use any motion information (our goal b)), thus the transition from one state to the next is modelled as Gaussian stochastic perturbations, also called a *non-motion model* [49].

For the implementation of the EKF we need to provide concrete values for Q_k, the Jacobian of h_k and R_k. The two latter ones are just the derivative of $h_k(x)$ and the variance of $h_k(x)$ when x is instantiated with a particular value, respectively, both already defined in our observation model. Regarding Q_k, under the *non-motion model* of transition it is known that[4] $Q_k = \widehat{v}^2_{max}/\chi^2_{1,\alpha}$ if the expected maximum speed of the system (the worker in this case) is $\widehat{v}_{max}$ with a probability of $1 - \alpha$. In our case we have chosen $0.5m/s$ as the maximum worker speed at all times with 95% of probability ($\alpha = 0.05$), thus we obtain $Q = 0.067$.

As for the discrete filter, it updates a posterior on a binary variable ($c_k \in \{\text{close}, \text{far}\}$) according to a recursive Bayesian formulation:

$$\underbrace{P(c_k|z_{1:k}, d_{1:k})}_{\text{posterior at } k} \propto \underbrace{p(z_k|c_k)}_{likelihood} \underbrace{\sum_{c_{k-1}} \underbrace{P(c_k|c_{k-1}, d_k)}_{transition} \underbrace{P(c_{k-1}|z_{1:k-1}, d_{1:k-1})}_{\text{posterior at } k-1}}_{prior} \tag{3}$$

In practice, between successive iterations of the filter we only have to store the posterior for $c_k = \text{close}$, since the belief in being far from the beacon is 1 minus that.

[4]The factor $\chi^2_{1,\alpha}$ is the value in the support of the chi-squared distribution with 1 degree of freedom that marks the beginning of an upper tail that has exactly an area of α.

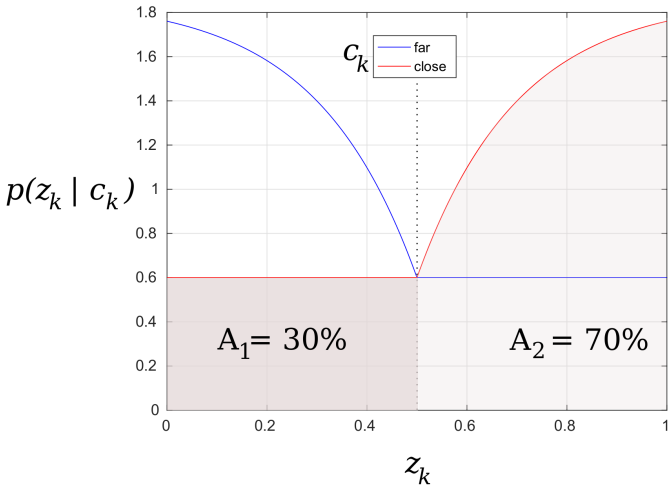

Figure 6: Likelihood function for the discrete filter, i.e., $p(z_k|c_k)$, for the two cases of c_k (worker far/close to the beacon = blue/red respectively).

The support of the likelihood probability distribution of this discrete filter is $z_k \in [0, 1]$, and we assume that c_k is known when evaluating it, i.e., the worker is believed to be either far or close to the beacon. Fig. 6 illustrates our definition of that likelihood. When we assume that the worker is close to the beacon, it is unlikely that the probability of being closer than τ_c is low ($z_k \in [0, 0.5]$), thus we have set a small uniform likelihood; in the same situation, observing higher and higher probabilities of being closer than τ_c to the beacon will be more and more likely, which, for the sake of a gradual evolution on those likelihoods, has been modelled as a first-order linear system response. The parameters of that first-order system response have been chosen to obtain an overall probability of getting large z_k of about 70% vs. a probability of observing small z_k of about 30%. The case of the worker being far from the beacon is naturally symmetric to this one (blue curve in the figure).

The transition of our discrete filter, $P(c_k|c_{k-1}, d_k)$, is a discrete *pmf* that depends on both the previous region and the current distance to the beacon. c_{k-1} will be instantiated with every possibility in the sum of eq. 3, but we do not know d_k (it is hidden); we use its estimate, produced by the EKF, instead, thus obtaining an approximation. For defining completely this approximate transition we use $P(c_k|c_{k-1})$ modulated by the evidence of

d_k, as follows: $P(c_k|c_{k-1})$ is increased linearly if the evidence provided by the estimate of d_k supports the particular combination of c_{k-1} and c_k, and is decreased linearly when that evidence contradicts it (it is not modified if $d_k = \tau_c$, the threshold we use to distinguish far from close). As for the values of $P(c_k|c_{k-1})$ needed to do these operations, we have filled in its 2 x 2 table after observing several experiments in which the worker passed by a beacon in a representative path; in these experiments the probability of changing from being close to the beacon to being far from the beacon in one measurement step is believed to be $3,23\%$, and the one of changing from far to close $0,72\%$. The other values of the $P(c_k|c_{k-1})$ table have been deduced from the fact that $\sum_{c_k} P(c_k|c_{k-1}) = 1, \quad \forall c_{k-1}$. Obviously, the mentioned values can be easily tuned for different environments and worker behaviours.

The final information needed to execute both filters is the prior distributions for d_0 and c_0. These are not critical either, since the filters usually converge in few steps. In the experiments shown in the next sections we have chosen values compatible with the scenarios, in particular for the worker being initially around $\pm 10cm$ from the true distance from the beacons with 95% probability and, consequently, in state $c_0 =$ far with 100% probability.

Fig. 7 shows the results obtained with our double continuous + discrete filter in a real scenario where a worker passes by a beacon twice. In spite of the noisy RSSI measurements, the EKF is able to track the true distance to the beacon quite well; more importantly, the noisy estimates of z_i red line in Fig. 7(b)), which only depend on the metrical distances d_i, are smoothed through the discrete filter, obtaining a quite robust and clean "closeness" signal (red line in Fig. 7(a)).

4.2. Status detection method

Based on the filtering process of subsection 4.1, we can detect whether the worker is going through risky situations. The minimum infrastructure for such detection is based on three different beacons as shown in figure 8. Beacons A and B are placed in the transition between a safe place and a risk area. A third beacon (C), located in the carabiner of the lifeline, is used to detect the connection between the harness, where the receiver is located, and the lifeline. The location of the worker with respect to the beacons is computed based on the output of the discrete filter described in subsection 4.1. That filter provides closeness detection in the form of a probability. We have used a reasonable threshold T (e.g. 0.75) on the belief of being close than τ_c to decide proximity to a particular beacon. If the status of the

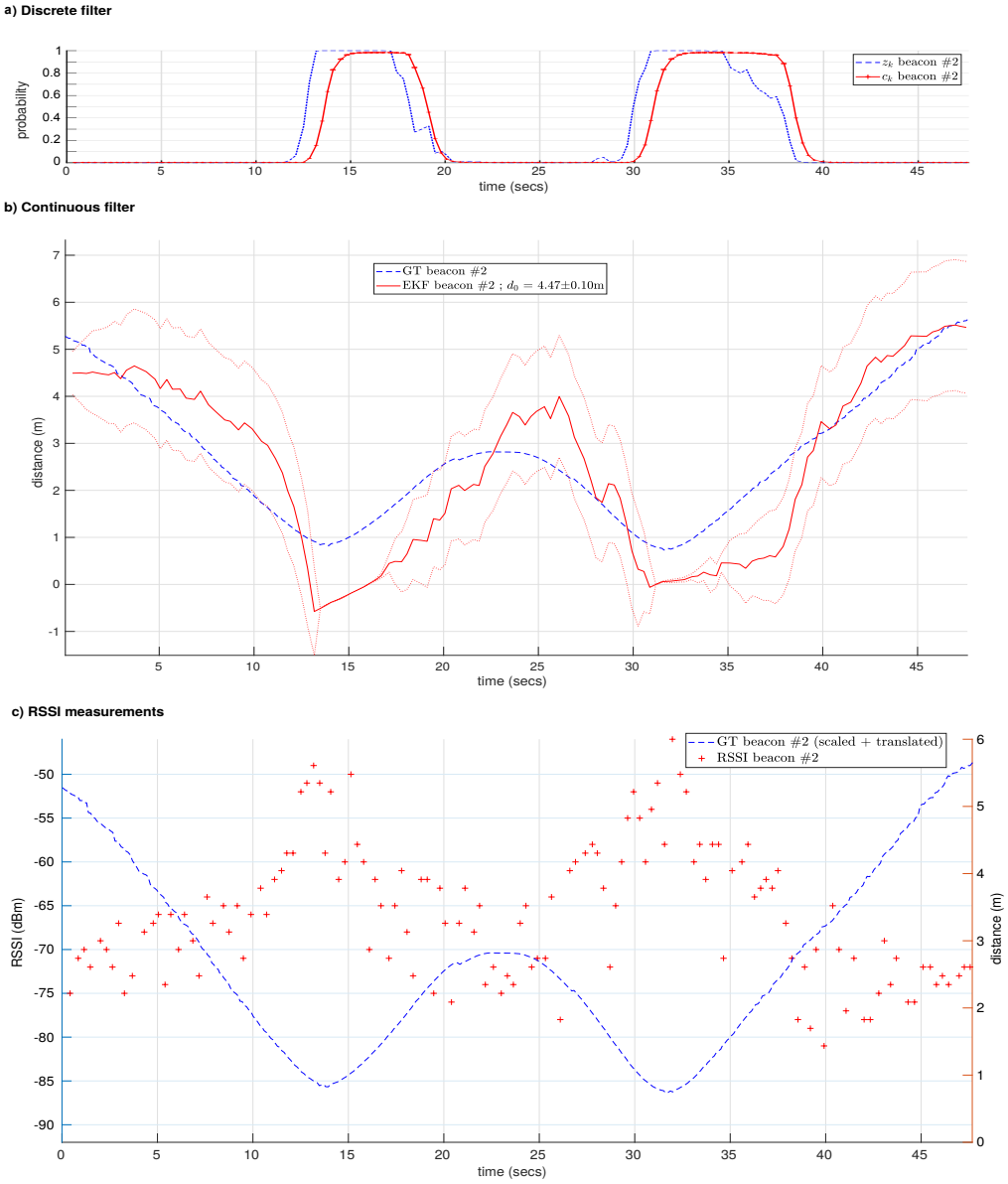

Figure 7: Results obtained by our double filter solution for estimating the "closeness" of the worker to a beacon. a) Estimates of z_i (blue) and c_i (red). b) EKF estimates of the metrical distance of the worker to the beacon (red) superimposed to the ground-truth provided by the LIDAR. c) RSSI measurements gathered along the worker path, who passes by the beacon twice (ground-truth estimates measured by the LIDAR are also superimposed for reference.

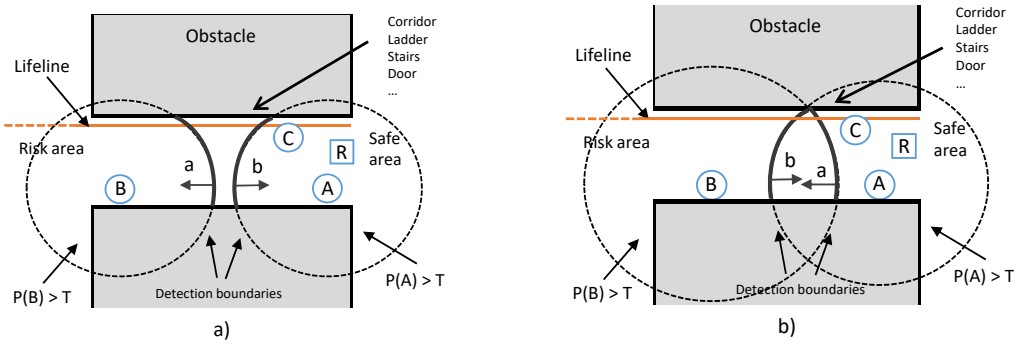

Figure 8: Beacons A and B placed in the transition between a safe place and a risk area. Beacon C is attached to the lifeline hook an the receiver (R) moves along the area. In a) A and B beacons have separated proximity areas delimited by the proximity threshold T. In b) beacons A and B have overlapped proximity areas.

last closeness decision is kept, large areas can be detected, as long as all the accesses are properly beaconized.

The distance between beacons A and B define whether proximity areas are separate or partially overlapped. In Figure 8a) beacons A and B have overlapped proximity areas, while in Figure 8b) areas are only partially overlapped. A distance between 1 and 2 m between beacons has been used in our experiments.

The worker status detection method can be modelled as a Finite State Machine (FSM) as shown in Figure 9. The detector has three states (0,1 and 2). The transition conditions are based on the output of the discrete filter presented in subsection 4.1 for each beacon.

Local notifications of the worker status are produced by using a red LED when the worker is in status 0 or 1, and with an acoustic signal when the worker status is 2.

4.3. Remote monitoring

Although local user notification and data logging of the status of the harness utilization works autonomously on the wearable receiver, additional external monitoring can also be included via IoT clients that offer real-time information of the state of every wearable in the construction site. In the absence of a Wi-Fi infrastructure, a cellular module (e.g. GPRS or 3G) can be

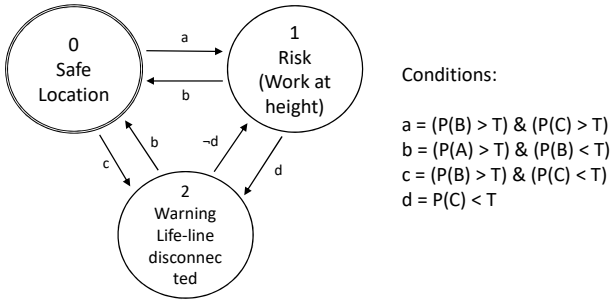

Figure 9: State diagram for the harness status identification FSM. Each transition is triggered by conditions a to d based on the filtered RSSI measurements from beacons A, B and C and the proximity signal threshold T.

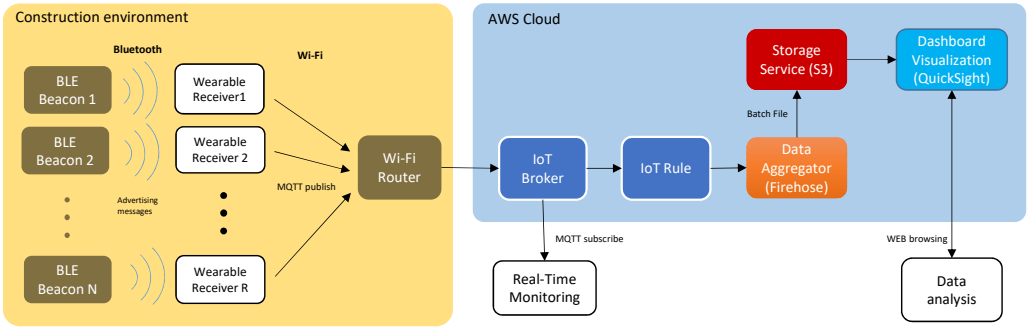

Figure 10: IoT architecture for the optional monitoring and data visualization of the receivers information.

added to the wearable and programmed using available PPP-over-Serial protocol (PPPoS) libraries. This way the wearable receiver publish the worker status to a IoT broker using an M2M lightweight protocol such as MQTT. Only status changes have to be published, thus reducing communications cost and power consumption.

For instance, monitoring dashboards of the IoT data (wearable locations, status and even RSSI data from every device) for further analysis can be built on the Amazon Web Services (AWS) platform using the *Quicksight* service. There, an IoT rule provides relevant MQTT messages to an aggregator (*Kinesis FireHose*) that store data sets in the *S3* storage service as shown in Figure 10.

5. Discussion of results

Three different scenarios have been tested to validate our method, where a worker with the wearable receiver walks along a 10 m by 2 m corridor that connects the safe area with the risky area, with different usage of the safety measures. Beacons A and B are placed in the middle section of the corridor with a separation of 2 m, located at a distance of 6 cm from the wall, and at a height of 115 cm from the floor. Transmitters were configured to advertise at intervals of 0.1 s. Beacon A is located at the safe side of the corridor, where the lifeline hook must be attached by the worker, while beacon B is located at the risky side, where the work at height begins.

The wearable receiver is fixed to the worker's safety harness, next to the carabiner. The third beacon (C) is installed on the lifeline hook lead (initially next to beacon A); that hook has to be attached to the harness with the wearable receiver, at all times, by the worker, while working at the risky side.

In order to get ground-truth data to validate and illustrate the results of our methods, an experimental setup has been built using an external computer and a LIDAR sensor on a wheeled platform, and a procedure to compute the distance between the receiver and the beacons has been programmed. The wheeled platform carries an inexpensive RPLidar A2 sensor by SlamTec[5], the BLE receiver and the computer. Measurements from the receiver and the LIDAR sensors have been synchronized and a Matlab script has been used to convert LIDAR scans into positions.

For each experiment, two graphs have been obtained; a time plot and a 2D plot of the path followed by the receiver. The time plot shows three types of data: raw RSSI measurements for each beacon; probability of proximity to each beacon; and results of the FSM, that gives the harness status based on the probabilities and a threshold.

The 2D path followed by the wearable receiver has been plotted over a map, with different sections and colours according to the harness status computed by the FSM described in section 4.2. Time labels have been added to match the changes in the closeness status with the time plot of the readings. A blue path indicates that the worker is in a safe area (state 0). Red indicates a risk area (state 1). Black has been used to indicate that the lifeline has been disconnected in a risk area (state 2).

[5]https://www.slamtec.com/en/Lidar/A2

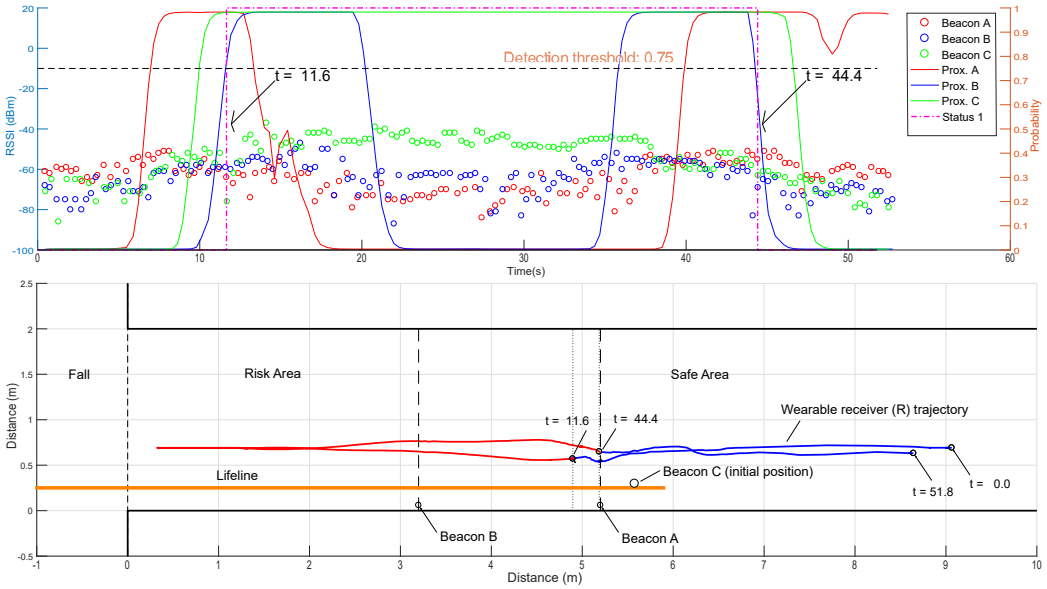

Figure 11: Scenario 1. The worker travels along the corridor attaching the harness at the beginning of the work at height and disconnecting it at the end. (Up) Raw RSSI data and output of the discrete filter. (Down) 2D trajectory of the worker on the corridor map.

5.1. Scenario 1. Proper use of the safety harness

In experiment 1 (see Figure 11), a proper use of PPE is shown, where the worker approaches beacon A and attaches the safety harness. Then he continues at a distance of approximately 70 cm from beacon B. The detection status is changed at T =11.6 s indicating that the worker is in the risk area, but with the safety measures on. After reaching the end of the corridor, he returns to beacon A in $T = 44.4\,s$, where the safety harness is disengaged from the lifeline carabiner.

5.2. Scenario 2. Harness disconnected in the middle of work at height

In experiment 2 (see Figure 12), a common, but illegal, use case is tested. Here, the worker attaches the lifeline by the beacon A, but the lifeline is temporary disconnected while working at the risk area. Once reconnected, the worker returns to the starting point and disengages the lifeline again. This situation was recognized as a normal case in $T = 16.0\,s$, but the violation

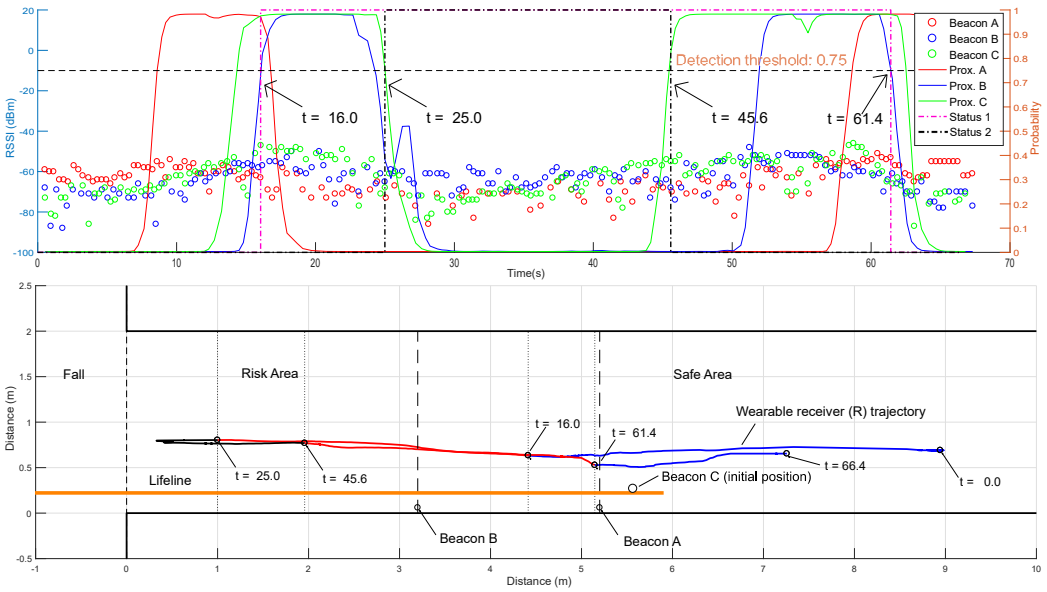

Figure 12: Scenario 2. Task where the harness is disconnected in the middle of work at height. (Up) Raw RSSI data and output of the discrete filter. (Down) Trajectory of the worker along the corridor map. The black section shows the illegal section in black.

is detected at $T = 25.0\,s$ until $T = 45.6\,s$. This has been shown in Figure 12(Down), where the risky path section is drawn in black.

In this case, acoustic local notification can be used to notify the worker and a log of events stored in the device can be analysed for later assessment of the use of PPE.

5.3. Scenario 3. Lifeline not used

Here (see Figure 13), the worker walks along the corridor, passing in front of the beacons A, B, and C at a distance of approximately 1 m without connecting the harness to the lifeline. The lifeline beacon (C) is detected twice, but as the worker moves away from it, the FSM changes the status to illegal (status 2) between $T = 15.4\,s$ and $T = 36.8\,s$.

6. Conclusions and future work

The system proposed in this paper, based on the use of BLE beacons for the location of workers in the workplace and of efficient statistical filtering

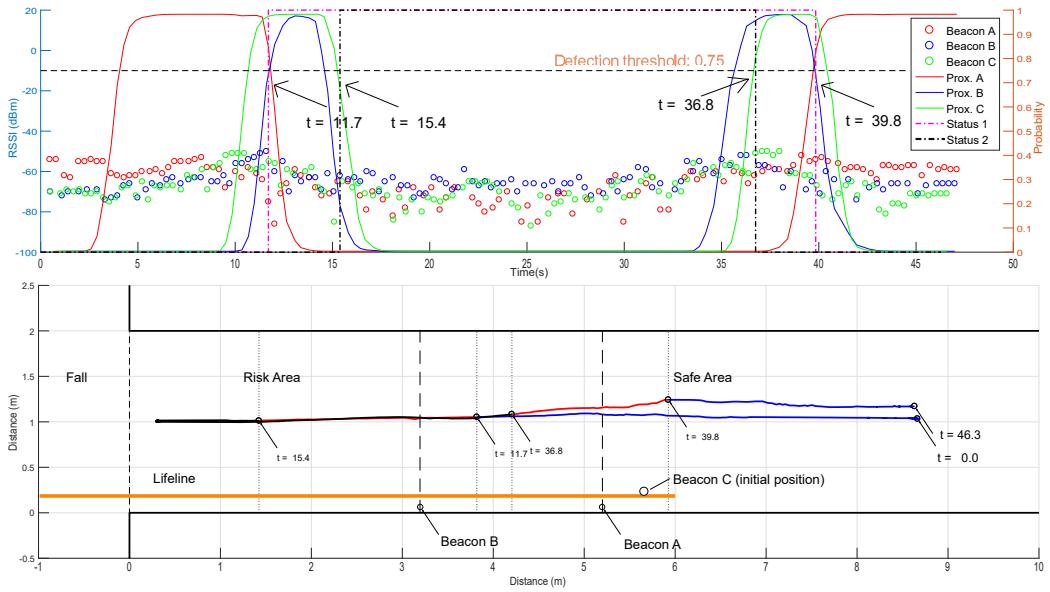

Figure 13: Scenario 3. Task example where the lifeline has no been connected to the harness. The lifeline beacon has been detected as the worker passes by, but the illegal status is detected when the worker enters the risk area. (Up) Raw RSSI data and output of the discrete filter. (Down) Trajectory of the worker along the corridor map

for processing their data, has been proved to be an effective tool for detecting robustly whether the worker is located in a place where harness and lifelines are mandatory and whether these are being used properly.

The system can be installed in corridors, stairs, ladders, etc., and requires minimum configuration and infrastructure (just tree beacons per boundary). There is no need for communications networks or maps, and can be easily relocated, making it ideal for very dynamic environments such as construction sites.

The experiments presented have been based on the minimum set of beacons, but this system can be applied to any number of areas and workers. The use of a special advertising ID for the A, B and C-type beacons allows us to create unlimited virtual boundaries without maps or configuration of the electronic devices. Special labelling or colour coding on the beacons can make this deployment easier. Also, accuracy can be improved by increasing the number of beacons in the system.

The maximum distance to the beacons that has been tested is around 1 m. Higher distances can be achieved by using multiple A-B beacons (e.g. in both walls of the corridor) or using antennas with higher gain. The distance between beacons has been chosen experimentally. In future work we have to study the use of shorter distances to reduce the transition distance for shorter corridors.

As the wearable receiver antenna varies the polarization angle against the transmitters antennas as the user moves, changes in the attenuation of the signals can occur for a given distance. Solutions using multiple receivers [51] with different orientations for RSSI stabilization are too bulky and would add too much complexity. The use of new compact MIMO antennas for Bluetooth [52] would reduce the multi-path propagation effects but do not avoid the attenuation caused by the human body proximity. In that sense, the use of multiple A-B beacons would help to get a more reliable estimation.

Our method not only provides local real-time detection of the use of harness by workers in zones designated as dangerous, but also allows for remote monitoring, which would provide improved coordination of safety conditions and proper execution of dangerous tasks. The (small) detection delay due to the causal filters for the local real-time detector can be removed when using RSSI data for remote off-line analysis. Remote control of the safety measures in real time can lead to improvements in safety conditions for dangerous tasks. Coordination and planning of tasks can be updated with real input from people working in dangerous zones.

According to the manufacturer, the beacon batteries can last for more than a year, and are easily replaceable. Moreover, as the receiver scan beacons messages in passive mode, a Li-Ion 18650 battery can last for more than one day without charging.

This method is a step toward the development of infrastructure-less or device-free methods in the future, as suggested by [38].

6.1. Impact on construction sector

The economic impact of our system is very small when compared with the total budget of the majority of construction projects. Cost of beacons and receptor range from 10 to 20 Euro per unit. Environmental impact is also low because beacons and receptors can be re-used once the works has been finished.

Traditionally, the construction sector has proved to be a sector resistant to the introduction of technological changes when compared with other industrial sectors. Support from company directors and management will be necessary to ensure successful implementation and use of the system proposed. Workers' privacy and the opposition of some workers to being located continuously could act as an obstacle. Considering the system as an effective safety tool could reduce initial resistance on the part of workers.

Acknowledgements

The authors would like to acknowledge the contribution from "Fundación Laboral De La Construcción" for allowing them to test the system on a real construction site, and also contributions from Andrés Ogáyar Flores, José Ramón Gámez Murcia and Daniel Casale Linde.

References

[1] A. Gibb, H. Lingard, M. Behm, T. Cooke, Construction accident causality: learning from different countries and differing consequences, Construction Management and Economics 32 (2014) 446–459.

[2] X. S. Dong, X. Wang, J. A. Largay, J. W. Platner, E. Stafford, C. T. Cain, S. D. Choi, Fatal falls in the us residential construction industry, American journal of industrial medicine 57 (2014) 992–1000.

[3] C. F. Chi, T. C. Chang, H. I. Ting, Accident patterns and prevention measures for fatal occupational falls in the construction industry, in: Applied Ergonomics, volume 36, Elsevier, 2005, pp. 391–400.

[4] M. A. C. López, D. O. Ritzel, I. Fontaneda, O. J. G. Alcantara, Construction industry accidents in spain, Journal of safety research 39 (2008) 497–507.

[5] Identifying elements of poor construction safety management in China, 2004.

[6] H. J. Im, Y. J. Kwon, S. G. Kim, Y. K. Kim, Y. S. Ju, H. P. Lee, The characteristics of fatal occupational injuries in Korea's construction industry, 1997-2004, Safety Science 47 (2009) 1159–1162.

[7] J. Dumrak, S. Mostafa, I. Kamardeen, R. Rameezdeen, Factors associated with the severity of construction accidents: The case of South Australia, Australasian Journal of Construction Economics and Building 13 (2013) 32.

[8] R. Irumba, Spatial analysis of construction accidents in Kampala, Uganda, Safety Science 64 (2014) 109–120.

[9] P. A. Schulte, R. Rinehart, A. Okun, C. L. Geraci, D. S. Heidel, National prevention through design (ptd) initiative, Journal of safety research 39 (2008) 115–121.

[10] M. D. M. Aires, M. C. R. Gámez, A. Gibb, Prevention through design: The effect of european directives on construction workplace accidents, Safety science 48 (2010) 248–258.

[11] J. A. Gambatese, M. Behm, S. Rajendran, Design's role in construction accident causality and prevention: Perspectives from an expert panel, Safety science 46 (2008) 675–691.

[12] M. Gangolells, M. Casals, N. Forcada, X. Roca, A. Fuertes, Mitigating construction safety risks using prevention through design, Journal of safety research 41 (2010) 107–122.

[13] S. Zhang, K. Sulankivi, M. Kiviniemi, I. Romo, C. M. Eastman, J. Teizer, Bim-based fall hazard identification and prevention in construction safety planning, Safety science 72 (2015) 31–45.

[14] J. Teizer, T. Cheng, Y. Fang, Location tracking and data visualization technology to advance construction ironworkers' education and training in safety and productivity, Automation in Construction 35 (2013) 53–68.

[15] C. Clevenger, C. Lopez del Puerto, S. Glick, Interactive bim-enabled safety training piloted in construction education., Advances in Engineering Education 4 (2015) n3.

[16] R. Navon, O. Kolton, Model for automated monitoring of fall hazards in building construction, Journal of Construction Engineering and Management 132 (2006) 733–740.

[17] E. Cheung, A. P. Chan, Rapid demountable platform (RDP) - A device for preventing fall from height accidents, 2012.

[18] S.-N. Min, J.-Y. Kim, M. Parnianpour, The effects of safety handrails and the heights of scaffolds on the subjective and objective evaluation of postural stability and cardiovascular stress in novice and expert construction workers, Applied ergonomics 43 (2012) 574–581.

[19] J. C. Rubio-Romero, M. C. R. Gámez, J. A. Carrillo-Castrillo, Analysis of the safety conditions of scaffolding on construction sites, Safety science 55 (2013) 160–164.

[20] J. C. Rubio-Romero, M. Rubio, C. García-Hernández, Analysis of construction equipment safety in temporary work at height, Journal of Construction Engineering and Management 139 (2012) 9–14.

[21] J. M. Adam, F. J. Pallarés, P. A. Calderón, Falls from height during the floor slab formwork of buildings: current situation in spain, Journal of safety research 40 (2009) 293–299.

[22] N. Craciun, The personal protective equipment against falls from height at the limit between risk and security, Calitatea 18 (2017) 140.

[23] B. H. Guo, Y. M. Goh, Ontology for design of active fall protection systems, Automation in Construction (2017).

[24] X. S. Dong, J. A. Largay, S. D. Choi, X. Wang, C. T. Cain, N. Romano, Fatal falls and pfas use in the construction industry: Findings from the niosh face reports, Accident Analysis & Prevention 102 (2017) 136–143.

[25] J. Song, C. T. Haas, C. Caldas, E. Ergen, B. Akinci, Automating the task of tracking the delivery and receipt of fabricated pipe spools in industrial projects, Automation in Construction 15 (2006) 166–177.

[26] C. H. Caldas, D. G. Torrent, C. T. Haas, Using Global Positioning System to Improve Materials-Locating Processes on Industrial Projects, Journal of Construction Engineering and Management 132 (2006) 741–749.

[27] J. Teizer, D. Lao, M. Sofer, Rapid automated monitoring of construction site activities using ultra-wideband, in: Proceedings of the 24th International Symposium on Automation and Robotics in Construction, Kochi, Kerala, India, pp. 19–21.

[28] W. Wu, H. Yang, D. A. Chew, S. hua Yang, A. G. Gibb, Q. Li, Towards an autonomous real-time tracking system of near-miss accidents on construction sites, Automation in Construction 19 (2010) 134–141.

[29] H. Yang, D. A. S. Chew, W. Wu, Z. Zhou, Q. Li, Design and implementation of an identification system in construction site safety for proactive accident prevention, Accident Analysis and Prevention 48 (2012) 193–203.

[30] A. Kelm, L. Laußat, A. Meins-Becker, D. Platz, M. J. Khazaee, A. M. Costin, M. Helmus, J. Teizer, Mobile passive Radio Frequency Identification (RFID) portal for automated and rapid control of Personal Protective Equipment (PPE) on construction sites, Automation in Construction 36 (2013) 38–52.

[31] C. Musu, V. Popescu, D. Giusto, Workplace safety monitoring using RFID sensors, in: 2014 22nd Telecommunications Forum Telfor (TELFOR), IEEE, 2014, pp. 656–659.

[32] S. Movassaghi, P. Arab, M. Abolhasan, Wireless technologies for Body Area Networks: Characteristics and challenges, in: 2012 International Symposium on Communications and Information Technologies (ISCIT), IEEE, 2012, pp. 42–47.

[33] N. Newman, Apple ibeacon technology briefing, Journal of Direct, Data and Digital Marketing Practice 15 (2014) 222–225.

[34] K. E. Jeon, J. She, P. Soonsawad, P. C. Ng, BLE Beacons for Internet of Things Applications: Survey, Challenges and Opportunities, 2017.

[35] E. Valero, A. Adán, Integration of rfid with other technologies in construction, Measurement 94 (2016) 614 – 620.

[36] R. Faragher, R. Harle, Location Fingerprinting With Bluetooth Low Energy Beacons, IEEE Journal on Selected Areas in Communications 33 (2015) 2418–2428.

[37] P. Lin, Q. Li, Q. Fan, X. Gao, Real-Time Monitoring System for Workers' Behaviour Analysis on a Large-Dam Construction Site, International Journal of Distributed Sensor Networks 9 (2013) 509423.

[38] J. Shang, X. Hu, F. Gu, D. Wang, S. Yu, Improvement Schemes for Indoor Mobile Location Estimation: A Survey, Mathematical Problems in Engineering 2015 (2015) 1–32.

[39] X. Li, J. Wang, C. Liu, A Bluetooth/PDR Integration Algorithm for an Indoor Positioning System, Sensors 15 (2015) 24862–24885.

[40] J. W. Park, X. Yang, Y. K. Cho, J. Seo, Improving dynamic proximity sensing and processing for smart work-zone safety, Automation in Construction 84 (2017) 111–120.

[41] P. Huang, L. Tsung-Han, C. Hao-hua, Method of reducing power consumption of a radio badge in a boundary detection localization system, 2009.

[42] T. H. Lin, P. Huang, H. H. Chu, C. W. You, Energy-efficient boundary detection for RF-based localization systems, IEEE Transactions on Mobile Computing 8 (2009) 29–40.

[43] M. D'Arco, A. Renga, A. Ceccarelli, F. Brancati, A. Bondavalli, Enhancing workers safety in worksites through augmented gnss sensors, Measurement 117 (2018) 144 – 152.

[44] J. Lindh, Bluetooth low energy beacons, Texas Instruments (2015) 2.

[45] Q. Dong, W. Dargie, Evaluation of the reliability of RSSI for indoor localization, 2012 International Conference on Wireless Communications in Underground and Confined Areas, ICWCUCA 2012 (2012) 2–7.

[46] M. Hata, Empirical formula for propagation loss in land mobile radio services, IEEE Transactions on Vehicular Technology 29 (1980) 317–325.

[47] R. Faragher, R. Harle, An Analysis of the Accuracy of Bluetooth Low Energy for Indoor Positioning Applications, Proceedings of the 27th International Technical Meeting of The Satellite Division of the Institute of Navigation (ION GNSS+ 2014) (2014) 201–210.

[48] T. Verma, J. Pearl, Causal networks: Semantics and expressiveness, in: Machine Intelligence and Pattern Recognition, volume 9, Elsevier, 1990, pp. 69–76.

[49] J.-A. Fernández-Madrigal, Simultaneous Localization and Mapping for Mobile Robots: Introduction and Methods: Introduction and Methods, IGI Global, 2012.

[50] G. L. Smith, S. F. Schmidt, L. A. McGee, Application of statistical filter theory to the optimal estimation of position and velocity on board a circumlunar vehicle, National Aeronautics and Space Administration, 1962.

[51] J. Rodas, T. M. Fernández, D. I. Iglesia, C. J. Escudero, Multiple antennas bluetooth system for rssi stabilization, in: 2007 4th International Symposium on Wireless Communication Systems, pp. 652–656.

[52] H. Hui-Fen, X. Shu-Guang, Compact mimo antenna for bluetooth, wimax, wlan, and uwb applications, Microwave and Optical Technology Letters 58 (2016) 783–787.